

This article was downloaded by:

On: 23 January 2011

Access details: *Access Details: Free Access*

Publisher *Taylor & Francis*

Informa Ltd Registered in England and Wales Registered Number: 1072954 Registered office: Mortimer House, 37-41 Mortimer Street, London W1T 3JH, UK



Journal of Coordination Chemistry

Publication details, including instructions for authors and subscription information:

<http://www.informaworld.com/smpp/title~content=t713455674>

New Au(III), Pt(II) and Pd(II) complexes with glycyyl-containing homopeptides

Bojidarka B. Koleva^a; Sonya Zareva^b; Tsonko Kolev^c; Michael Spiteller^c

^a Lehrstuhl für Analytische Chemie, Ruhr-Universität Bochum, Universitätsstraße 150, 44780 Bochum, Germany ^b Sofia University, 1164 Sofia, Bulgaria ^c Institut für Umweltforschung, Universität Dortmund, 44221 Dortmund, Germany

To cite this Article Koleva, Bojidarka B. , Zareva, Sonya , Kolev, Tsonko and Spiteller, Michael(2008) 'New Au(III), Pt(II) and Pd(II) complexes with glycyyl-containing homopeptides', *Journal of Coordination Chemistry*, 61: 22, 3534 – 3548

To link to this Article: DOI: 10.1080/00958970802108817

URL: <http://dx.doi.org/10.1080/00958970802108817>

PLEASE SCROLL DOWN FOR ARTICLE

Full terms and conditions of use: <http://www.informaworld.com/terms-and-conditions-of-access.pdf>

This article may be used for research, teaching and private study purposes. Any substantial or systematic reproduction, re-distribution, re-selling, loan or sub-licensing, systematic supply or distribution in any form to anyone is expressly forbidden.

The publisher does not give any warranty express or implied or make any representation that the contents will be complete or accurate or up to date. The accuracy of any instructions, formulae and drug doses should be independently verified with primary sources. The publisher shall not be liable for any loss, actions, claims, proceedings, demand or costs or damages whatsoever or howsoever caused arising directly or indirectly in connection with or arising out of the use of this material.

New Au(III), Pt(II) and Pd(II) complexes with glycylic-containing homopeptides

BOJIDARKA B. KOLEVA*[†], SONYA ZAREVA[‡],
TSONKO KOLEV[§] and MICHAEL SPITELLER[§]

[†]Lehrstuhl für Analytische Chemie, Ruhr-Universität Bochum,
Universitätsstraße 150, 44780 Bochum, Germany

[‡]Sofia University, St. Kl. Ohridski", 1, J. Bourchier blvd., 1164 Sofia, Bulgaria

[§]Institut für Umweltforschung, Universität Dortmund,
Otto-Hahn-Strasse 6, 44221 Dortmund, Germany

(Received 30 November 2007; in final form 4 February 2008)

Twelve new Au(III), Pt(II) and Pd(II) complexes with glycylic-containing homopeptides glycylic-glycine (G2), glycylic-glycyl-glycine (G3), glycylic-glycyl-glycyl-glycine (G4), glycylic-glycyl-glycyl-glycyl-glycine (G5) and glycylic-glycyl-glycyl-glycyl-glycyl-glycine (G6) have been synthesized, isolated and characterized spectroscopically and structurally by means of solid-state linear-dichroic infrared (IR-LD) spectroscopy of oriented colloids in nematic liquid crystal host, ¹H- and ¹³C-NMR, TGA and DSC, UV-Vis spectroscopy, EPR, ESI- and FAB mass spectrometry and HPLC tandem mass spectrometry (HPLC-MS/MS). Quantum chemical calculations are carried out with a view to obtain the structures and spectroscopic properties of the ligand and newly synthesized metal complexes.

Keywords: Glycylic-containing homopeptides; Au(III); Pd(II); Pt(II); *Cisplatin*; Complexes, Solid-state linear polarized IR-spectroscopy; UV-Vis; EPR; Quantum chemical calculations; ¹H- and ¹³C NMR; ESI MS; TGA and DSC; HPLC-MS-MS

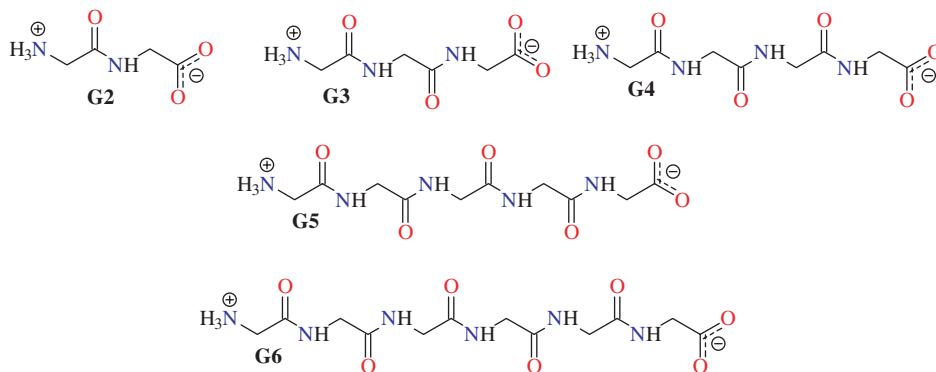
1. Introduction

The remarkable clinical success of *cis*-Pt(NH₃)₂Cl₂ for treatment of a variety of cancers made it an archetypal inorganic drug [1, 2]. Although a large number of patients have been cured after *cisplatin* treatment of cancer, the facts are that the precise mechanism of actions remains elusive and that severe side effects develop after administration of the treatment [2–9]. This has opened up research areas for development of new Pt(II) complexes, mainly varying the types of the ligands, and creating new anticancer drugs with minimal side effects [10–14]. Another area of investigation is coordination of Au(III) with organic ligands and developing potential anticancer medications with Au(III) as the active ion [15–20]. Au(III) has a configuration isoelectronic with Pt(II), and therefore was among the first non-Pt metals explored for antitumor potential. Similar to Pt(II) complexes, Au(III) compounds are able to bind to DNA perhaps

*Corresponding author. Email: BKoleva@chem.uni-sofia.bg

accounting for their cytotoxic activity. A key problem that hampered the development of Au(III) complexes is their low stability under physiological conditions. Au(III) compounds are highly oxidative and able to oxidize biomolecules such as methionine and glycine. The stability of Au(III) compounds can be enhanced by chelating ligands. Examples include Au(III) complexes with bipyridine containing ligands [15–20] and quinoline derivatives [21]. The newly synthesized Au(III) complexes have been reported to be appreciably stable under physiological conditions and to have antiproliferative properties against selected human tumor cell lines [15–20, 21]. Peptides are appropriate ligands for development of the new anticancer medications both with Pt(II) and Au(III). In a series of papers the coordination ability of these metal ions with small peptides has been investigated [22–28]. Only three crystal structures of Au(III) peptide complexes [22, 23] are known, two with dipeptide glycylhistidine ($[\text{Au}(\text{H-Gly-L-His-OH})\text{H}_{-1}]\text{Cl}]\text{Cl}\cdot 3\text{H}_2\text{O}$) and $[\text{Au}(\text{H-Gly-L-His-OH})\text{H}_{-3}]_4\cdot 10\text{H}_2\text{O}$ and one with tripeptide glycylglycylhistidine $[\text{Au}(\text{H-Gly-Gly-His-OH})\text{H}_{-2}]\text{Cl}\cdot \text{H}_2\text{O}$, obtained in strong acidic medium. For the first complex *in vivo* activity has shown that the complex is fairly cytotoxic towards the established A2780 ovarian carcinoma human cell line either sensitive or resistant to *cisplatin* [29]. Remarkably, the complex has been found far more cytotoxic than the corresponding Zn(II), Pd(II), Pt(II) and Co(II) complexes implying that cytotoxicity is related to the presence of a Au(III) center [29], encouraging further investigation of coordination of Au(III) with peptides.

Herein as a part of our systematic spectroscopic and structural elucidation of metal complexes with peptides as potential anticancer medications, we report twelve new Au(III), Pt(II) and Pd(II) complexes with glycyl-containing homopeptides glycyl-glycine (G2), glycyl-glycyl-glycine (G3), glycyl-glycyl-glycyl-glycine (G4), glycyl-glycyl-glycyl-glycyl-glycine (G5) and glycyl-glycyl-glycyl-glycyl-glycyl-glycine (G6), depicted in scheme 1. Their structures and spectroscopic properties are elucidated by solid-state linear-dichroic (IR-LD) infrared spectroscopy of oriented colloids in nematic liquid crystal host, ^1H - and ^{13}C -NMR, TGA and DSC, UV-Vis spectroscopy, ESI- and FAB mass spectrometry and HPLC with tandem mass spectrometry (HPLC-MS/MS). The successful application of IR-LD for direct evidence of coordination ability is demonstrated on these systems, where the impossibility for isolation of suitable single



Scheme 1. Diagram of glycyl-containing homopeptides glycyl-glycine (G2), glycyl-glycyl-glycine (G3), glycyl-glycyl-glycyl-glycine (G4), glycyl-glycyl-glycyl-glycyl-glycine (G5) and glycyl-glycyl-glycyl-glycyl-glycyl-glycine (G6).

crystals prevent single crystal X-ray diffraction as a structural method. Quantum chemical calculations are carried out to obtain the structures and spectroscopic parameters of the G5 and G6 ligands and all of the complexes studied. Coordination with Pd(II) are reference investigations due to Pd(II) interacting quicker with peptide systems.

2. Experimental

2.1. Materials and methods

IR spectra were measured on a THERMO NEXUS FTIR-spectrometer (4000–400 cm^{-1} , 1 cm^{-1} resolution, 200 scans) equipped with a Specac wire-grid polarizer. The non-polarized solid-state IR spectra were recorded using KBr disk technique. The oriented samples were obtained as a colloid suspension in a nematic host (ZLI 1695, Merck) using the technique described [30–33]. The validation of the orientation method [32] for accuracy, precision and the influence of the liquid crystal medium on peak positions and integral absorbances of the guest molecule bands, as well as the optimization of experimental conditions and an experimental design for quantitative evaluation of the impact of four input factors, have been presented [32]. The number of scans, the rubbing-out of KBr-pellets, the amount of studied compounds included in the liquid crystal medium and the ratios of Lorentzian to Gaussian peak functions in the curve fitting procedure on the spectroscopic signal at five different frequencies has been studied [32]. Procedures for the position (ν_i) and integral absorbancies (A_i) determination for each i -peak have been carried out by deconvolution and curve-fitting procedures at 50 : 50% ratio of Lorentzian to Gaussian peak functions, χ^2 factors within 0.00066–0.00019 and 2000 iterations [32]. The means of two treatments were compared by Student t -test. The experimental IR-spectral patterns have been acquired and processed by GRAMS/AI 7.01 IR spectroscopy (Thermo Galactic, USA) and STATISTICA for Windows 5.0 (StatSoft, Inc., Tulsa, OK, USA) program packages. The nature and balance of the forces in the nematic liquid crystal suspension system, the mathematical model for their clearance, morphology of the suspended particles and the influence of the space system types on the degree of orientation i.e. ordering parameter has been shown [36] using five liquid crystals and fifteen compounds. Applicability of the last approach for experimental IR-spectroscopic band assignment and especially for obtaining structural information has been demonstrated in a series of organic systems and metal complexes [34], Cu(II) complexes [35], polymorphs [36], codeine derivatives [37], peptides with their Au(III) complexes, hydrochlorides and hydrogensquarates [38–40].

HPLC-MS/MS analysis. Analyses of the samples were performed with a Thermo Finnigan surveyor LC-Pump. Compounds were separated on a Luna C18 column (150 × 2 mm, 4 μm particle size) from Phenomenex (Torrance, CA, USA). The mobile phase consisted of water +0.1% HCOOH (A) and acetonitrile +0.1% HCOOH (B) using a gradient program presented in table 1. The compound was detected via UV and a TSQ 7000 (Thermo Electron Corporation, Dreieich, Germany) mass spectrometer. The spectra were obtained using the TSQ 7000 equipped with an ESI ion source and operated with the following conditions: capillary temperature 180°C; sheath gas 60 psi

Table 1. Characteristic IR-bands of neutral peptides (G2–G6 according to scheme 1) and their Au(III), Pt(II) and Pd(II) complexes.

Assignment	ν [cm ⁻¹]				
	G2 [39]	Au(III)-G2	G3 [39]	Au(III)-G2	Pt(II)-G3
$\nu_{\text{NH}_2}^{\text{as}}, \nu_{\text{NH}_2}^{\text{s}}$	—	3322, 3274, 2120	—	3316, 3162	3307, 3000
ν_{NH}	3288	—	3316, 3298	—	—
$\nu_{\text{NH}_3+}^{\text{as}}, \nu_{\text{NH}_3+}^{\text{s}}$	3200 – 2400	—	3200 – 2400	—	—
$\nu_{\text{C=O}}$	—	1740	—	1733	1728
$\delta_{\text{NH}_3+}^{\text{as}}$	1679, 1673	—	—	1681, 1621	—
δ_{NH_2}	—	1660	—	1643	1655
$\nu_{\text{C=O}}$ (Amide I)	1656	1685	1657, 1646	1683, 1666	1689, 1676
$\nu_{\text{COO-}}^{\text{as}}$	1533	—	1534	—	—
δ_{NH} (Amide II)	1554	—	1556, 1519	—	—
$\delta_{\text{NH}_3+}^{\text{s}}$	1500	—	1506	—	—
$\nu_{\text{COO-}}^{\text{s}}$	1409	—	1400	—	—
ν_{CN} (Amide III)	1253	1216	1228	1222	1200
γ_{NH} (Amide V)	713	—	696, 690	—	—
$\delta_{\text{C=O}}$ (Amide IV)	663	563	644, 640	700, 698	723, 678
$\gamma_{\text{C=O}}$ (Amide VI)	532	588	570, 561	590, 577	588, 531
	G4 [39]	Au(III)-G4	Pt(II)-G4	Pd(II)-G4	
$\nu_{\text{NH}_2}^{\text{as}}, \nu_{\text{NH}_2}^{\text{s}}$	—	3300, 3180	3271, 3222	3214, 3200	
ν_{NH}	3335, 3294, 3283	3100	3300	3297	
$\nu_{\text{NH}_3+}^{\text{as}}, \nu_{\text{NH}_3+}^{\text{s}}$	3200 – 2400	—	—	—	
$\nu_{\text{C=O}}$	—	1733	1728	1735	
$\delta_{\text{NH}_3+}^{\text{as}}$	1675, 1688	—	—	—	
δ_{NH_2}	—	1656	1662	1660	
$\nu_{\text{C=O}}$ (Amide I)	1662, 1646, 1638	1680, 1666, 1642	1673, 1670, 1663	1683, 1677, 1660	
$\nu_{\text{COO-}}^{\text{as}}$	1563	—	—	—	
δ_{NH} (Amide II)	1579, 1554, 1535	—	—	—	
$\delta_{\text{NH}_3+}^{\text{s}}$	1469	—	—	—	
$\nu_{\text{COO-}}^{\text{as}}$	1415	—	—	—	
ν_{CN} (Amide III)	1245 with submaxima	1216 with submaxima	1233 broad	1240	
γ_{NH} (Amide V)	719, 699, 683	—	—	—	
$\delta_{\text{C=O}}$ (Amide IV)	667, 651, 647,	560, 555, 640	560, 554, 530	555, 540, 543	

(Continued)

Table 1. Continued.

Assignment	ν [cm ⁻¹]					
	G2 [39]	Au(III)-G2	G3 [39]	Au(III)-G2	Pt(II)-G3	Pt(II)-G3
$\gamma_{\text{C=O}}$ (Amide VI)	611, 590, 582	580, 543, 518	590, 572, 564	591, 590, 577		
$\nu_{\text{NH}_2}^{\text{as}}, \nu_{\text{NH}_2}^{\text{s}}$	—	3304, 3295	3367, 3360	3322, 3278		
ν_{NH}	3302, 3298, 3284, 3269	3267	3300	3200		
$\nu_{\text{NH}_3^+}^{\text{as}}, \nu_{\text{NH}_3^+}^{\text{s}}$	3100 – 2500	—	—	—		
$\nu_{\text{C=O}}$	—	1720	1737	1717		
$\delta_{\text{NH}_3^+}^{\text{as}}$	1698, 1688	—	—	—		
δ_{NH_2}	—	1650	1684	1689		
$\nu_{\text{C=O}}$ (Amide I)	1684, 1674, 1659, 1632	1680, 1666, 1642, 1630	1688, 1660, 1644, 1639	1677, 1647, 1641, 1640		
ν_{COO^-}	1563	—	—	—		
δ_{NH} (Amide II)	1578, 1568, 1561, 1541	1532	1542	1515		
$\delta_{\text{NH}_3^+}^{\text{as}}$	1529	—	—	—		
$\nu_{\text{COO}^-}^{\text{as}}$	1413	—	—	—		
ν_{CN} (Amide III)	1252	1216 broad	—	—		
ν_{NH} (Amide V)	727, 722, 713, 700	703	1233 with submaxima 700 broad	1241 with submaxima 722 broad		
$\delta_{\text{C=O}}$ (Amide IV)	681, 666, 614, 610	560, 555, 640, 660	577, 562, 532, 500	590, 588, 579, 542		
$\gamma_{\text{C=O}}$ (Amide VI)	557, 535, 512, 510	577, 540, 533, 525	589, 576, 555, 534	623, 600, 592, 568		
		G6	Pt(II)-G6	Pd(II)-G6		
$\nu_{\text{NH}_2}^{\text{as}}, \nu_{\text{NH}_2}^{\text{s}}$	—	3311, 3280, 3098	3300, 3296	3318, 3277, 3100		
ν_{NH}	3332, 3327, 3310, 3300, 3275	3211, 3210	3310, 3316	3343, 3330		
$\nu_{\text{NH}_3^+}^{\text{as}}, \nu_{\text{NH}_3^+}^{\text{s}}$	3200 – 2400	—	—	—		
$\nu_{\text{C=O}}$	—	1716	1733	1722		
$\delta_{\text{NH}_3^+}^{\text{as}}$	1690, 1689	—	—	—		
δ_{NH_2}	—	1671	1682	16712		
$\nu_{\text{C=O}}$ (Amide I)	1686, 1676, 1660, 1635, 1627	1689, 1677, 1670, 1664, 1650	1688, 1672, 1677, 1670, 1668	1680, 1677, 1672, 1661, 1660		
$\nu_{\text{COO}^-}^{\text{as}}$	1560	—	—	—		
δ_{NH} (Amide II)	1548, 1537, 1524, 1513, 1502	1552, 1550	1513, 1525	1526, 1521		
$\delta_{\text{NH}_3^+}^{\text{as}}$	1527	—	—	—		
$\nu_{\text{COO}^-}^{\text{as}}$	1405	—	—	—		
ν_{CN} (Amide III)	1288	1264 series of peaks	About 1264	—		
ν_{NH} (Amide V)	727, 720, 692, 694, 672	Broad band with submaxima about 700	≈700	1264, 1261, 1260, 1254, 1257		
$\delta_{\text{C=O}}$ (Amide IV)	684, 681, 677, 673, 666	Broad band with submaxima about 610	≈600	700, 699, 683, 670, 662		
$\gamma_{\text{C=O}}$ (Amide VI)	582, 580, 578, 561, 541	Broad band with submaxima about 550	≈530	600, 540, 523, 520, 511 530, 517, 210, 501, 500		

and spray voltage 4.5 kV. 1 mg mL^{-1} of the sample was dissolved in acetonitrile and injected into the ion source by an auto sampler (Finnigan Surveyor). Using the Excalibur 1.4 software the data obtained was processed.

^1H - and ^{13}C -NMR measurements, reference sodium 3-(trimethylsilyl)-tetradeuteropropionate, were made at 298 K with a Bruker DRX-400 spectrometer using 5 mm tubes and $\text{D}_2\text{O}/\text{H}_2\text{O}$ as solvent mixture at ratio 9 : 1.

Optimization of the structures of zwitterionic G5 and G6 were carried out by *ab initio* calculations (RHF) at 6-31++G** basis set using Dalton 2.0 and GAUSSIAN 98 program packages [41, 42]. The visualization of the output files is done by ChemCraft 5.0 [43]. The methodology [44] for exploring the conformational energy landscape [44, 45] was used. The scheme first creates all possible conformers by rotating around the flexible bonds according to suitable step size and then employs a hierarchy of increasingly more accurate electronic structure methods. For every structure the stationary points found on the potential energy hypersurfaces were characterized using standard analytical harmonic vibrational analysis. The absence of imaginary frequencies, as well as negative eigenvalues of the second-derivative matrix, confirmed that the stationary points correspond to minima on the potential energy hypersurfaces. Calculation of vibrational frequencies and infrared intensities were checked to establish which kind of performed calculations agree best with the experimental data. Geometries of the metal complexes were optimized by the DFT method with the B3LYP functional. We ascertained that the optimized geometries did not exhibit any imaginary frequency except for the geometries that were optimized under constraints. Energy and population changes were evaluated with the DFT, MP2 to MP4(SDQ), and CCSD(T) methods. In the CCSD(T) calculation, the contribution of triple excitations was incorporated noniteratively with single and double excitation wave functions. The basis set system described below was mainly used for the calculation. For Pd, the MIDI-4 basis set was used, where one diffuse d function ($\xi=0.124$) was added and the 5p orbitals were represented by the same exponents and the same coefficients as those of the 5s orbital. For Pt and Au, the standard LANL2DZ basis set was used for geometry optimization, where the basis sets and ECPs for the other atoms were taken to be the same as those employed for the Pd system.

Elemental analyses were carried out according to standard procedures for C and H (as CO_2 and H_2O) and N (by the Dumas method). The thermogravimetry was carried out using a Perkin-Elmer TGS2 instrument. Calorimetry was performed on a DSC-2C Perkin Elmer apparatus under argon.

X-band EPR spectra are measured on a BRUKER ESR 300 spectrometer in methanol at 298 K.

2.2. Synthesis

The Au(III), Pd(II) and Pt(II) complexes of the peptides listed in the scheme were obtained from equimolar aqueous solutions of the ligands with corresponding metal salts, $\text{HAuCl}_4 \cdot 2\text{H}_2\text{O}$ (Merck, 0.3737 g), PdCl_2 (Merck, 0.1773 g) or *cis*- $\text{Pt}(\text{NH}_3)_2\text{Cl}_2$ (0.3000 g, Sigma Aldrich). Thus, obtained solutions are continuously stirred and heated at 40°C for 10–20 h. The pH values are kept in the range 5.5–6.0 by dropwise addition of 0.001 M NaOH. When pH values are within 6.5–8.5, Au(III) is reduced to Au(II) with UV–Vis absorption maximum at 510 nm. These solutions are EPR active due to

Au(II), $5d^9$ and $S=1/2$. The EPR spectra at room temperature show four hyperfine lines of ^{197}Au and $g_0 = 2.006\text{--}2.003$ ($A_0^{\text{Au}} = 40.01\text{--}42.16 \cdot 10^{-4} \text{ cm}^{-1}$). With pH 8.5–10.0 after a day gold film is obtained. Precipitates from the newly synthesized complexes are obtained after a week (Pd(II) complexes, orange), 20 days (Pt(II) complexes, white) and a month (Au(III) complexes, white). All are filtered off, washed with water and dried in air at room temperature. The Pd(II) and Pt(II) complexes are stable in ambient conditions for more than 2.0 months, while the Au(III) complex turns to black precipitate (reduction of Au(III) to Au(0)) after 2.0–2.2 months. In all cases, the yield of precipitate is within 10–35%. Elemental analysis of: (i) Complexes with G2, Found: C, 13.22; H, 1.59; N, 7.68; $[\text{AuC}_4\text{H}_6\text{N}_2\text{O}_3\text{Cl}]$ Calcd: C, 13.25; H, 1.67; N, 7.74%, (ii) Complexes with G3, Found: C, 18.80; H, 2.07; N, 11.02; $[\text{AuC}_6\text{H}_9\text{N}_3\text{O}_4]$ Calcd: C, 18.81; H, 2.10; N, 10.97%; Found: C, 17.88; H, 2.00; N, 10.55; $[\text{PtC}_6\text{H}_8\text{N}_3\text{O}_4]\text{Na}$ Calcd: C, 17.83; H, 1.99; N, 10.40%; (ii) Complexes with G4, Found: C, 21.88; H, 2.55; N, 12.70; $[\text{AuC}_8\text{H}_{11}\text{N}_4\text{O}_5]$ Calcd: C, 21.83; H, 2.52; N, 12.73%, Found: C, 20.87; H, 2.40; N, 12.78; $[\text{PtC}_8\text{H}_{11}\text{N}_4\text{O}_5]\text{Na}$ Calcd: C, 20.83; H, 2.40; N, 12.73%, Found: C, 25.82; H, 3.00; N, 15.00; $[\text{PdC}_8\text{H}_{11}\text{N}_4\text{O}_5]\text{Na}$ Calcd: C, 25.79; H, 2.98; N, 15.04%; (iii) Complexes with G5, Found: C, 26.10; H, 2.88; N, 14.00; $[\text{AuC}_{10}\text{H}_{14}\text{N}_5\text{O}_6]$ Calcd: C, 26.16; H, 2.84; N, 14.09%, Found: C, 23.73; H, 2.77; N, 13.55; $[\text{PtC}_{10}\text{H}_{14}\text{N}_5\text{O}_6]\text{Na}$ Calcd: C, 23.17; H, 2.72; N, 13.51%, Found: C, 27.96; H, 3.31; N, 16.37; $[\text{PdC}_{10}\text{H}_{14}\text{N}_5\text{O}_6]\text{Na}$ Calcd: C, 27.95; H, 3.28; N, 16.30%; (iv) Complexes with G6, Found: C, 26.05; H, 3.00; N, 15.17; $[\text{AuC}_{12}\text{H}_{17}\text{N}_6\text{O}_7]$ Calcd: C, 26.00; H, 3.09; N, 15.16%, Found: C, 25.04; H, 2.99; N, 14.52; $[\text{PtC}_{12}\text{H}_{17}\text{N}_6\text{O}_7]\text{Na}$ Calcd: C, 25.05; H, 2.98; N, 14.61%, Found: C, 29.66; H, 3.55; N, 17.29; $[\text{PdC}_{12}\text{H}_{17}\text{N}_6\text{O}_7]\text{Na}$ Calcd: C, 29.61; H, 3.52; N, 17.28%.

3. Results and discussion

3.1. Conventional and linear polarized IR-spectroscopic data

Evidence for coordination of G2, G3 and G4 as the NH-amide deprotonated ligands was obtained from comparison (table 1) of IR-spectra of corresponding Au(III), Pt(II) and Pd(II) complexes with these of the free ligands [39] showing disappearance of amide ν_{NH} and δ_{NH} stretching and bending peaks as well as high frequency shifting of amide I. The new $\nu_{\text{C=O}}$ bands over 1700 cm^{-1} in both complexes toward the protonated forms of the peptides [39] show coordination of metal ions (III) via O-atom from COO^- -group and a C=O double bond formation. The absence of characteristic NH_3^+ bands in the ligands IR-spectra and an observation of stretching ($\nu_{\text{NH}_2}^{\text{as}}$ and $\nu_{\text{NH}_2}^{\text{s}}$) and bending (δ_{NH_2}) ones for NH_2 group, with values typical for coordinated primary NH_2 -group supported including of $\text{N}_{(\text{amino})}$ inside the coordination sphere. In the case of the G4 complexes, observation of the $\nu_{\text{C=O}}$ stretching band at 1725 cm^{-1} is attributed to formation of COOH during coordination. A difference of $\Delta\nu_{\text{C=O}}$ of about 15 cm^{-1} is observed monodentate carboxylate. The application of reducing-difference procedure to polarized IR-spectra of the complexes gives elimination of amide I peak/s and $\nu_{\text{C=O}}$ in different dichroic ratios (figure 1). The data assume a cross-oriented disposition of corresponding transition moments, supporting the predicted structures. The confirmation of δ_{NH_2} and $\nu_{\text{NH}_2}^{\text{s}}$ (table 1) origin arises from the observed simultaneous elimination

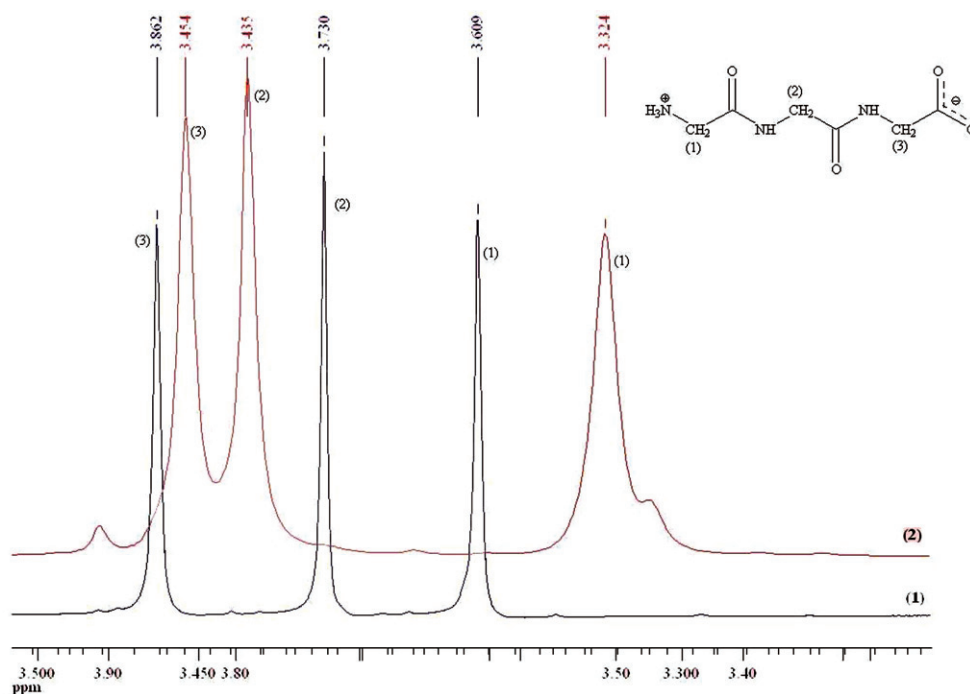


Figure 1. ¹H-NMR spectrum of G3 (1) and its Au(III)-complex (2).

of corresponding peaks due to their co-linear orientation in the frame of one structural fragment. Fermi-resonance split $\nu_{\text{NH}_2}^s$ in the Au(III)-complex with G2 is explained with the asymmetric intermolecular H-bonding with participation of NH₂-group [24–28].

The IR-spectroscopic characterization of metal complexes with G5 and G6 by comparison between IR spectra of the ligands and coordination compounds started with the IR-band assignment of the penta- and hexapeptides. IR-spectra of both the ligands are shown in Supplemental Material. The overlapping of the characteristic maxima requires the application of deconvolution and curve fitting procedure for data interpretation [39]. The obtained peaks and their assignments are listed in table 1. The δ_{NH} values are typical for *trans* amide fragments where the frequency of the IR-band corresponding to δ_{NH} (Amide II) is observed between 1560–1530 cm⁻¹ [39]. Application of the reduced difference procedure for polarized IR-LD spectra allow confirmation of *trans* configuration of the amide fragments in both peptides due to elimination of each Amide I band (table 1) and corresponding ν_{NH} peaks within the 3300–3250 cm⁻¹ region. Similar to the other complexes, coordination with metal leads to disappearance of some characteristics for amide O=C–NH groups. For G5 and G6 only one and corresponding two ν_{NH} , δ_{NH} and γ_{NH} frequencies are observed. The elimination of the bands of ν_{NH} in all of the complexes with G5 and G6 leads to disappearance of the peaks at 1630 cm⁻¹ (Au(III) complex), 1639 cm⁻¹ (Pt(II) complex), 1640 cm⁻¹ (Pd(II) complex) and at 1650, 1664 cm⁻¹ (Au(III) complex), 1670, 1668 cm⁻¹ (Pt(II) complex) and 1661, 1660 cm⁻¹ (Pd(II) complex) proving that coordination with the metal in these peptides keeps the *trans*-configuration of the amide groups not influenced by coordination (scheme 3). Other changes in the IR characteristics are similar to the other cases and support the coordination shown in scheme 3 (table 1).

3.2. ^1H - and ^{13}C -NMR data

^1H -NMR chemical shifts of CH_2 ($\text{N}_{(\text{termini})}$) and CH_2 ($\text{C}_{(\text{termini})}$) proton signals in the Au(III) complex with G2 are at 3.455, 3.870, 3.860 and 3.853 ppm. Similar chemical shift differences $\Delta\delta$ of +0.405 and -0.017 ppm have been obtained for Pd(II) and Pt(II) ($[\text{MLH}_{-1}\text{Cl}]^-$) complexes H-Gly-Gly-OH [46, 47]. The data suppose $[\text{Au(III)LH}_{-1}\text{Cl}]$ complex formation and tridentate coordination of the ligand via COO^- , NH-amide and NH_2 -groups. The ^{13}C -NMR data agree with CH_2 ($\text{N}_{(\text{termini})}$) and CH_2 ($\text{C}_{(\text{termini})}$) carbon chemical shifts of 41.56 ppm and 39.78 ppm, upfield with $\Delta\delta = -0.781$ and 0.890 ppm. The COO^- signal is shifted downfield to 182.00 ppm ($\Delta\delta = 12.91$ ppm).

^1H -NMR data of Au(III) and Pt(II) complexes with G3 indicate formation of $[\text{MLH}_{-2}]$ as $\text{CH}_2(3)$, $\text{CH}_2(2)$ and $\text{CH}_2(1)$ signals are upfield with $\Delta\delta = -0.285$, -0.200 , -0.295 , -0.288 , -0.408 and -0.404 ppm (figure 1). ^{13}C -NMR chemical shifts of the ligand show peaks at 175.45 (CO(3)), 170.54 (CO(2)), 166.54 (CO(1)), 44.11 ($\text{CH}_2(3)$), 43.07 ($\text{CH}_2(2)$) and 41.02 ($\text{CH}_2(1)$) [20, 21]. In both complexes, an upfield shift of all the signals, $\Delta\delta$ within -2.45 to -2.30 , -0.89 to -0.82 and -0.93 to -0.910 ppm, are obtained. The downfield shifting of COO^- signal ($\Delta\delta = 10.68$ and 9.17 ppm) confirms coordination via COO^- . Similar data are obtained for Ni(II) and Pd(II) complexes of G3 ($[\text{M(II)LH}_{-2}]^-$) [48, 49] with a tetradentate coordination via COO^- , both NH amide and NH_2 -group.

For G4, G5 and G6 complexes with Au(III), Pt(II) and Pd(II) (Supplemental Material) the coordination affected chemical signals for $\text{gly}_1\text{-gly}_4$ and $\text{gly}_1\text{-gly}_5$ $-\text{CH}_2$ protons in the ranges of 4.0 – 3.5 ppm. In the complexes with G4–G6 like in the previous cases, the $\Delta\delta$ differences within 0.288 to 0.212, -0.29 to -0.288 and -0.411 to -0.400 ppm indicated coordination started with the $\text{N}_{(\text{termini})}$. ^{13}C -NMR chemical shifts of the ligands show peak differences, $\Delta\delta$, within about 2.5, 0.7, 0.9, 0.7 (G4), as well as additional changes of 0.77 (G5) and 0.55 (G6). The observed downfield shifting of COO^- signals, $\Delta\delta = 0.68$ (G4), 1.2 (G5) and 0.7 (G6), typical for protonated peptides [39, 40], show that during the complexation with these peptides protonation of COOH occurs.

3.3. HPLC MS-MS, ESI-MS and FAB-MS data

The HPLC separation of Au(III), Pd(II) and Pt(II) complexes with all of the peptides are characterized with dependences of relative abundance versus time (t). In all cases the observed peaks for singly charged $[\text{C}_4\text{H}_9\text{N}_2\text{O}_3]^+$, $[\text{C}_6\text{H}_{11}\text{N}_3\text{O}_4]^+$, $[\text{C}_8\text{H}_{15}\text{N}_4\text{O}_5]^+$, $[\text{C}_{10}\text{H}_{17}\text{N}_5\text{O}_6]^+$ and $[\text{C}_{12}\text{H}_{20}\text{N}_6\text{O}_7]^+$ ions about m/z 133.0 ± 0.2 , 190.0 ± 0.1 , 247.00 ± 0.3 , 304.00 ± 0.1 and 361.00 ± 0.1 of the free peptides explains the low yield obtained for coordination compounds. For Au(III) complex of G2 (Supplemental Material) the HPLC-MS-MS data give a peak at m/z 361.15 ($t = 4.02$) corresponding to $[\text{C}_4\text{H}_9\text{N}_2\text{O}_3\text{AuCl}]^+$ with molecular weight of 362.5. In complexes of Au(III) and Pt(II) with G3 peaks in the HPLC-MS-MS spectra are observed at m/z 385.3 ($t = 5.06$) and 384.8 ($t = 4.00$) corresponding to $[\text{C}_6\text{H}_{12}\text{N}_3\text{O}_4\text{Au}]^+$ and $[\text{C}_6\text{H}_{13}\text{N}_3\text{O}_4\text{Pt}]^+$ with molecular weights of 385.12 and 384.24, respectively. Complex formation of G4 with metal ions is proved by the HPLC-MS-MS data, where peaks at m/z 440.3 ($t = 4.08$), 440.1 ($t = 4.11$) and 351.3 ($t = 5.20$) correspond to $[\text{C}_8\text{H}_{15}\text{N}_4\text{O}_5\text{Au}]^+$, $[\text{C}_8\text{H}_{17}\text{N}_4\text{O}_5\text{Pt}]^+$ and $[\text{C}_8\text{H}_{17}\text{N}_4\text{O}_5\text{Pd}]^+$ with molecular weights of 440.16, 440.29 and 351.61, respectively. Mass spectra of the G5 complexes with Au(III), Pt(II) and Pd(II) metal ions show peaks

at m/z 498.7 ($t = 11.4$) and 497.2 ($t = 10.6$) for the first two metal ions. These data are assigned to $[\text{C}_{10}\text{H}_{19}\text{N}_5\text{O}_6\text{Au}]^+$ and $[\text{C}_{10}\text{H}_{20}\text{N}_5\text{O}_6\text{Pt}]^+$ with molecular weights of 498.21 and 497.32, respectively. For Pd(II) complex the HPLC-MS-MS data (Supplemental Material) show the peak at 445.12 ($t = 4.03$) corresponding to the 2NH_4^+ adduct of $[\text{C}_{10}\text{H}_{20}\text{N}_5\text{O}_6\text{Pd}]^+$ with molecular weight of 407.66. The Na^+ and NH_4^+ adducts are typical for ESI-MS and for that reason analysis of peptides and their derivatives is preferable with a combination of HPLC-MS-MS [50–53]. In the cases of the metal complexes with G6, the discussed phenomenon is observed in all of the cases. The mass spectral data show peaks at m/z 602.12 ($t = 5.70$), 571.23 ($t = 4.55$) and 505.07 (Supplemental Material), corresponding to NH_4^+ or 2NH_4^+ adducts of $[\text{C}_{12}\text{H}_{21}\text{N}_6\text{O}_7\text{Au}]^+$, $[\text{C}_{12}\text{H}_{23}\text{N}_6\text{O}_7\text{Pt}]^+$ and $[\text{C}_{12}\text{H}_{23}\text{N}_6\text{O}_7\text{Pd}]^+$ with molecular weights of 554.26, 553.38 and 464.72, respectively.

3.4. UV–Vis spectroscopy

The UV–Vis spectra of Au(III), Pt(II) and Pd(II) complexes of peptides (figure 2) have absorption bands within 300–350 nm and ϵ 800–980 $\text{l mol}^{-1} \cdot \text{cm}^{-1}$. The observed maxima are assigned to ligand to metal charge transfer (CT) bands, which correlates with the e values. Observation of absorption bands about 245 nm corresponds to tridentate coordination of the Ac-peptides with Pt(II) [54–57]. In our case the band is bathochromic shifted more than 50 nm due to the participation of more than two deprotonated amide N -atoms and primary amino groups in the polydentate chelation with the metal. The CT bands of the Au(III) and Pd(II) have decreasing intensity (about 20%) in comparison with corresponding Pt(II) complex and an additional bathochromic shift of the bands of 15–25 nm.

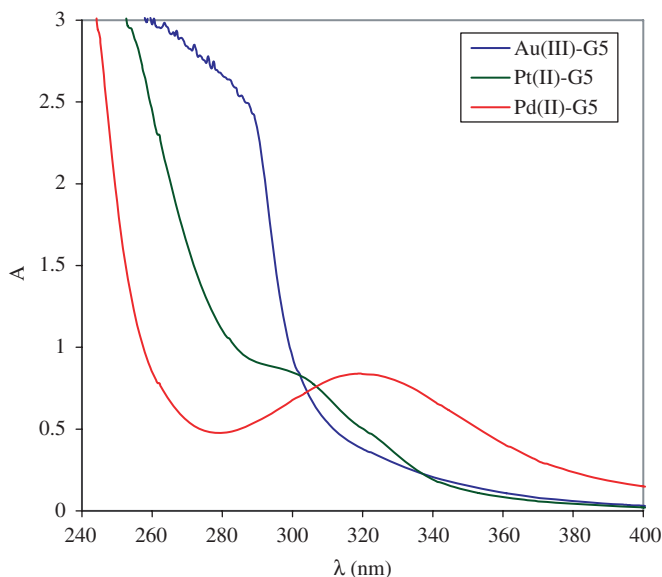


Figure 2. UV–Vis spectra Au(III), Pd(II) and Pt(II) complexes with G5.

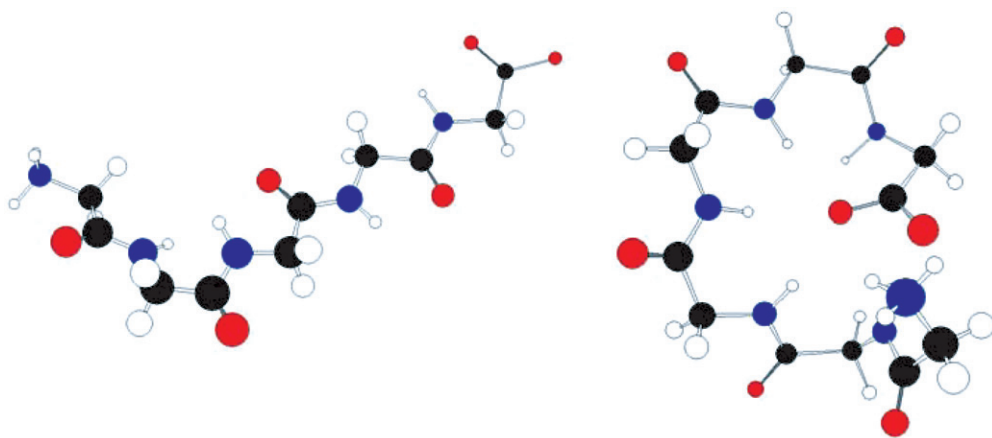
3.5. TGA and DSC data

TGA and DSC data within the range 300–500 K show that no solvent molecules are included in the Au(III), Pd(II) and Pt(II) complexes with the glycyI-containing homopeptides.

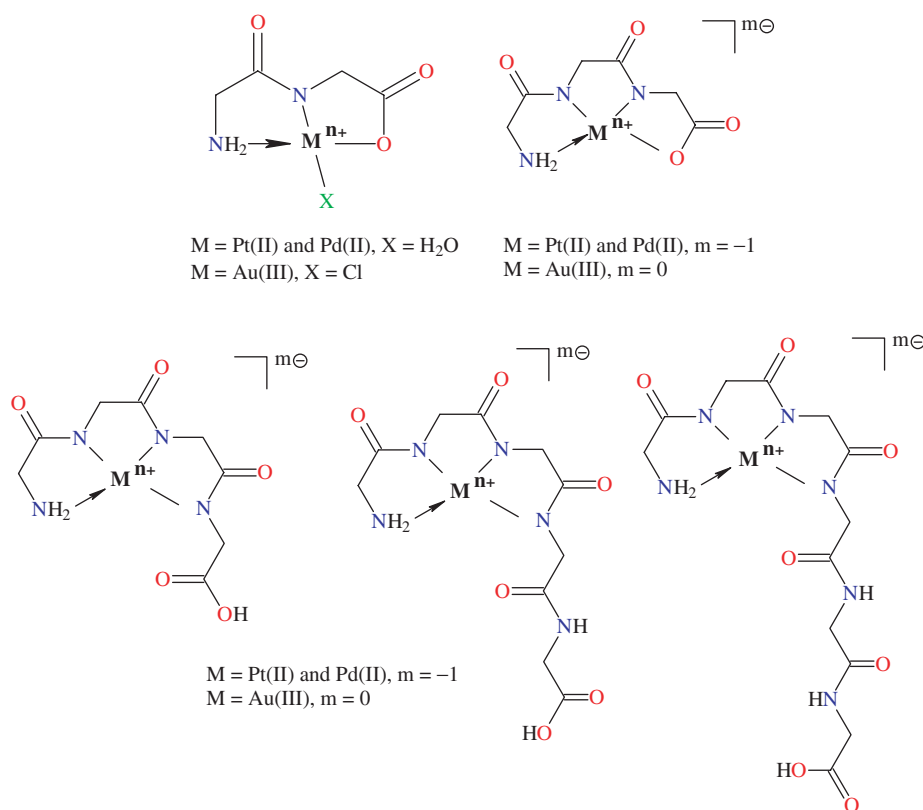
3.6. Theoretical calculations

Stable conformers of di, tri and tetrapeptides were reported [39], with detailed IR-LD spectroscopic characterization. Here we present the conformational analysis of penta- and hexahomopeptides (scheme 1). The conformational search on G5 and G6 (Supplemental Material) show a series of stable conformers with E_{rel} less than 10 kJ mol^{-1} . The most stable conformers of G5 and G6 with E_{rel} of 0.2 and 0.9 kJ mol^{-1} , respectively, are shown in scheme 2. In G5 an extended structure of the molecule is predicted, in accord with those of G2–G4 [39]. However, in G6 an element of cyclization is proposed with stable intermolecular hydrogen bonding ($\text{NH}_3^+ \cdots \text{OCO}$, bond length of 2.058 \AA). In both molecules the amide $\text{O}=\text{C}-\text{NH}$ groups are *trans* with dihedral angles within $177.1(6)$ – $179.0(2)^\circ$ for G5 and $175.1(6)$ – $180.0(0)^\circ$ for G6.

The input files for calculation of geometries of the complexes used the spectroscopic data for the proposed structures (scheme 3). The optimized geometries (scheme 4) and obtained values for selected bond lengths and angles in the AuN_2OCl , MN_3O ($\text{M} = \text{Au(III)}$ and Pd(II)) and MN_4 ($\text{M} = \text{Au(III)}$, Pt(II) and Pd(II)) chromophores in the complexes with G2, G3 and G4–G6 are within the ranges of $\text{M}-\text{NH}_2$, $\text{M}-\text{N}$ and $\text{M}-\text{O}$ bond lengths as well as $\text{N}-\text{M}-\text{N}$ and $\text{N}-\text{M}-\text{O}$ angles ($\text{M} = \text{Au(III)}$, Pd(II) and Pt(II)) are within 2.000 – 2.004 \AA , 1.955 – 2.000 \AA , 2.144 – 2.130 \AA and 89.0 – 100.1° , respectively. For all cases distortion of the flat square configuration of the metal ions is obtained. The deviation of planarity varies within 0.8 – 2.4° , 1.3 – 2.2° and 1.6 – 9.0° for Au(III) , Pd(II) and Pt(III) complexes, respectively. The obtained values of the geometric parameters correlated well with those experimentally obtained for peptide complexes with Au(III) , Pd(II) and Pt(II) by single crystal X-ray diffraction. According to literature data the $\text{M}-\text{NH}_2$, $\text{M}-\text{N}$ and $\text{M}-\text{O}$ bond lengths, as well as



Scheme 2. Most stable conformers of G5 and G6 at MP2/6-311++G** level of theoretical approximation.

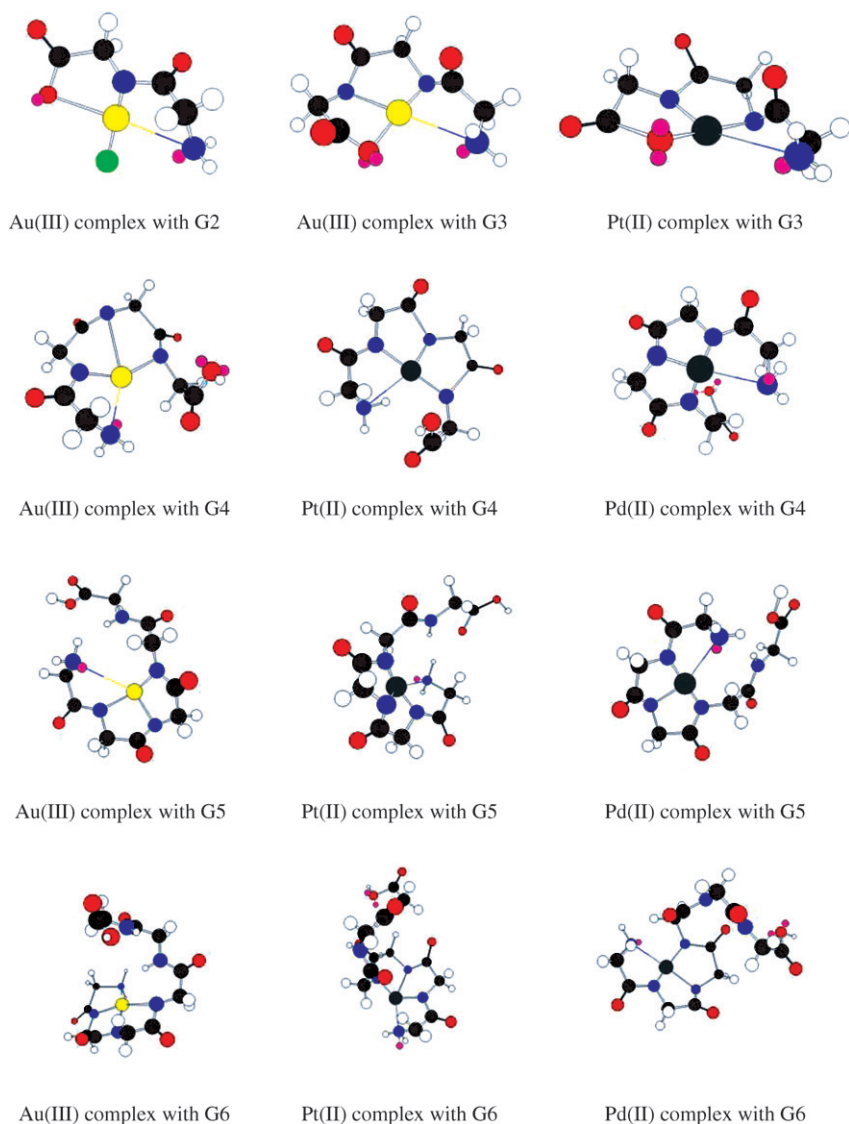


Scheme 3. Manner of coordination of Au(III), Pt(II) and Pd(II) with the glycyl-containing homopeptides.

N–M–N and N–M–O angles ($M = \text{Au(III)}, \text{Pd(II)}$ and Pt(II)), are within 2.024–2.013 Å, 1.935–2.003 Å, 2.157–2.143 Å and 89.6–101.4°, respectively [19, 20, 58–60].

4. Conclusion

The coordination ability of Au(III), Pt(II) and Pd(II) with glycyl-containing homopeptides glycyl-glycine, glycyl-glycyl-glycine, glycyl-glycyl-glycyl-glycine, glycyl-glycyl-glycyl-glycyl-glycine and glycyl-glycyl-glycyl-glycyl-glycyl-glycine is elucidated both in solution and in solid-state by means of solid-state IR-LD spectroscopy of oriented colloids in nematic liquid crystal host, ^1H - and ^{13}C -NMR, TGA and DSC, UV–Vis spectroscopy, EPR, ESI- and FAB mass spectrometry and HPLC tandem mass spectrometry (HPLC-MS/MS). The structures and spectroscopic properties of the ligands and twelve new metal complexes are predicted by quantum chemical calculations. Dipeptide coordinates in a tridentate manner with Au(III) via an O–atom (COO^-), *N*-amide nitrogen, after a previous deprotonation of the NH and NH_2 nitrogen. One Cl^- is attached to Au(III), yielding a planar geometry for the AuN_2OCl . The tripeptide is tetradentate towards Au(III) and Pt(II) through COO^- and two *N*-amide nitrogens, after deprotonation of the NH-groups and *N* atom from the



Scheme 4. Theoretically optimized geometries of the Au(III), Pd(II) and Pt(II) complexes with peptides studied.

–NH₂ fragment. Tetra-, penta- and hexapeptides are tridentate ligands with Au(III), Pt(II) and Pd(II) by their NH₂– and three deprotonated amide *N*-groups, yielding MN₄ chromophores with near square-planar geometry.

Acknowledgements

B.K. wishes to thank the Alexander von Humboldt Foundation for the Fellowship and Prof. W.S. Sheldrick for the useful and creative discussion. T.K. and M.S. wish to thank

the DAAD for a grant within the priority program "Stability Pact South-Eastern Europe" and the Alexander von Humboldt Foundation.

References

- [1] S. Komeda, M. Lutz, A. Spek, M. Chikuma, J. Reedijk. *J. Inorg. Chem.*, **39**, 4230 (2000).
- [2] J. Reedijk. *Chem. Commun.*, 801 (1996).
- [3] J. Reedijk. *Chem. Rev.*, **99**, 2499 (1999).
- [4] S. Van Zutphen, J. Reedijk., *Coord. Chem. Rev.*, **249**, 2845 (2005).
- [5] J.L. Van der Veer, G.A. Van der Marel, H. Van den Elst, J. Reedijk. *Inorg. Chem.*, **26**, 2272 (1987).
- [6] S. Van Boom, B. Chen, J. Teuben, J. Reedijk. *Inorg. Chem.*, **38**, 1450 (1999).
- [7] S. Komeda, M. Lutz, A. Spek, Y. Yamanaka, T. Sato, M. Chikuma, J. Reedijk. *J. Am. Chem. Soc.*, **124**, 4738 (2002).
- [8] B. Lippert (Ed.). *Cisplatin: Chemistry and Biochemistry of a Leading Anticancer Drug*, Wiley-VCH, Weinheim (1999).
- [9] T. Yang, C. Tu, J. Zhang, L. Lin, X. Zhang, L. Qin, J. Ding, Q. Xu, Z. Guo. *Dalton Trans.*, 3419 (2003).
- [10] E. Pantoja, A. Gallipoli, S. Van Zutphen, S. Komeda, R. Reddy, D. Jaganyi, M. Lutz, D. Tooke, A. Spek, C. Navarro-Ranninger, J. Reedijk. *J. Inorg. Biochem.*, **100**, 1955 (2006).
- [11] S. Van Rijt, S. Van Zutphen, H. Den Dulk, J. Brouwer, J. Reedijk. *Inorg. Chim. Acta*, **359**, 359 (2006).
- [12] S. Teletchea, S. Komeda, J. Teuben, M. Elizondo-Riojas, J. Reedijk, J. Kozelka. *Chem.-A Europ. J.*, **12**, 3741 (2006).
- [13] A. Magistrato, P. Ruggerone, K. Spiegel, P. Carloni, J. Reedijk. *J. Phys. Chem.*, **110B**, 3604 (2006).
- [14] A. Casini, G. Mastrobuoni, C. Temperini, C. Gabbiani, S. Francese, G. Moneti, G. Supuran, T. Claudiu, A. Scozzafava, L. Messori. *Chem. Commun.*, 156 (2007).
- [15] C. Gabbiani, A. Casini, L. Messori. *Gold Bulletin*, **40**, 73 (2007).
- [16] L. Messori, C. Gabbiani. *Metal Comp. Cancer Chemother.*, 355 (2005).
- [17] L. Messori, G. Marcon, M. Cinellu, M. Agostina, M. Coronello, E. Mini, C. Gabbiani, Q. Chiara, P. Orioli, P. Pierluigi. *Bioorg. Med. Chem.*, **12**, 6039 (2004).
- [18] L. Messori, G. Marcon. *Met. Ions Biol. Syst.*, 42 (2004).
- [19] L. Messori, G. Marcon, P. Orioli. *Bioinorg. Chem. Appl.*, **1**, 177 (2003).
- [20] G. Marcon, L. Messori, P. Orioli. *Exp. Rev. Anticancer Ther.*, **2**, 337 (2002).
- [21] T. Yang, C. Tu, J. Zhang, L. Lin, X. Zhang, Q. Liu, J. Ding, Q. Xu, Y. Guo, Y. Dalton *Trans.*, 3419 (2003).
- [22] S. Best, T. Chattopadhyay, M. Djuran, R. Palmer, P. Sadler, I. Sovago, K. Varnagy. *Dalton Trans.*, 2587 (1997).
- [23] M. Wienken, B. Lippert, E. Zangrando, L. Randaccio. *Inorg. Chem.*, **31**, 1983 (1992).
- [24] B.B. Ivanova. *J. Coord. Chem.*, **58**, 587 (2005).
- [25] B.B. Koleva, T. Kolev, S. Zareva, M. Spiteller. *J. Mol. Struct.*, **831**, 165 (2007).
- [26] T. Kolev, B. Ivanova, S. Zareva. *J. Coord. Chem.*, **60**, 109 (2007).
- [27] T. Kolev, S. Zareva, B. Koleva, M. Spiteller. *Inorg. Chim. Acta*, **359**, 4367 (2006).
- [28] B. Koleva, T. Kolev, M. Spiteller. *Inorg. Chim. Acta*, (2006), <http://dx.doi.org/10.1016/j.ica.2006.11.002>.
- [29] S. Carotti, G. Marcon, M. Marussich, T. Mazzei, L. Messori, E. Mini, P. Orioli. *Chem.-Biol. Interac.*, **125**, 29 (2000).
- [30] B.B. Ivanova, M. Arnaudov, P. Bontchev. *Spectrochim. Acta*, **60**, 855 (2004).
- [31] B.B. Ivanova, D.L. Tsalev, M. Arnaudov. *Talanta*, **69**, 822 (2006).
- [32] B. Ivanova, V. Simeonov, M. Arnaudov, D. Tsalev. *Spectrochim. Acta*, **67A**, 66 (2007).
- [33] B. Koleva, T. Kolev, T. Spassov, M. Spiteller. *Colloids Surf.* (2007), Submitted.
- [34] B.B. Ivanova. *Spectrochim. Acta*, **65A**, 5 (2005).
- [35] B. Ivanova, H. Mayer-Figge. *J. Coord. Chem.*, **58**, 653 (2005).
- [36] B. Ivanova. *J. Mol. Struct.*, **738**, 233 (2005).
- [37] R. Bakalska, B. Ivanova, T. Kolev. *Cent. Eur. J. Chem.*, **4**, 533 (2006).
- [38] B. Ivanova. *J. Mol. Struct.*, **782**, 122 (2006).
- [39] B. Ivanova, T. Kolev, S. Zareva. *Biopolymers*, **82**, 587 (2006).
- [40] T. Kolev. *Biopolymers*, **83**, 39 (2006).
- [41] M.J. Frisch, G.W. Trucks, H.B. Schlegel, G.E. Scuseria, M.A. Robb, J.R. Cheeseman, V.G. Zakrzewski, J.A. Montgomery Jr., R.E. Stratmann, J.C. Burant, S. Dapprich, J.M. Millam, A.D. Daniels, K.N. Kudin, M.C. Strain, Ö. Farkas, J. Tomasi, V. Barone, M. Cossi, R. Cammi, B. Mennucci, C. Pomelli, C. Adamo, S. Clifford, J. Ochterski, G.A. Petersson, P.Y. Ayala, Q. Cui, K. Morokuma, P. Salvador, J.J. Dannenberg, D.K. Malick, A.D. Rabuck, K. Raghavachari, J.B. Foresman,

- J. Cioslowski, J.V. Ortiz, A.G. Baboul, B.B. Stefanov, G. Liu, A. Liashenko, P. Piskorz, I. Komáromi, R. Gomperts, R.L. Martin, D.J. Fox, T. Keith, M.A. Al-Laham, C.Y. Peng, A. Nanayakkara, M. Challacombe, P.M.W. Gill, B. Johnson, W. Chen, M.W. Wong, J.L. Andres, C. Gonzalez, M. Head-Gordon, E.S. Replogle, J.A. Pople. *Gaussian 98*, Gaussian, Inc., Pittsburgh, PA (1998).
- [42] DALTON, a molecular electronic structure program, Release 2.0 (2005), <http://www.kjemi.uio.no/software/dalton/dalton.html>
- [43] G.A. Zhurko, D.A. Zhurko. ChemCraft: Tool for treatment of chemical data, Lite version build 08 (freeware), 2005.
- [44] D. Toroz, T. Van Mourik. *Mol. Phys.*, **105**, 209 (2007).
- [45] D. Toroz, T. Van Mourik. *Mol. Phys.*, **104**, 559 (2006).
- [46] V. Aletras, N. Hadjiliadis, A. Karatiota, I. Rombeck, B. Lippert. *Inorg. Chim. Acta*, **277**, 17 (1994).
- [47] A. Odani, Sh. Deguchi, O. Yamauchi. *Inorg. Chem.*, **25**, 62 (1986).
- [48] C.G. Agoston, T. Jankowska, I. Sovago. *Dalton Trans.*, 3295 (1999).
- [49] J. Slocik, R.E. Sphepherd. *Inorg. Chim. Acta*, **311**, 80 (2000).
- [50] A. Siebert, W.S. Sheldrick. *Dalton Trans.*, 385 (1997).
- [51] C. Frohling, W.S. Sheldrick. *Dalton Trans.*, 4411 (1997).
- [52] D. Wolters, W.S. Sheldrick. *Dalton Trans.*, 1121 (1999).
- [53] S. Manka, F. Becker, O. Hohage, W.S. Sheldrick. *J. Inorg. Biochem.*, **98**, 1947 (2004).
- [54] D. Morgan, M. Bursey. *J. Mass Spectrom.*, **30**, 473 (1995).
- [55] Y. Wang, F. Ke, K.W.M. Siu, R. Guevremont. *J. Mass Spectrom.*, **31**, 34 (1996).
- [56] D. Morgan, M. Bursey. *J. Mass Spectrom.*, **30**, 290 (1995).
- [57] S. Carr, C. Cassidy. *J. Mass Spectrom.*, **32**, 959 (1997).
- [58] T. Yang, C. Tu, J. Zhang, L. Lin, H. Zhang, Q. Liu, Q. Ding, Z. Xu, Z. Guo. *Dalton Trans.*, 3419 (2003).
- [59] S. Milinkovic, T. Parac, M. Djuran, N. Kostic. *Dalton Trans.*, 2771 (1997).
- [60] D. Shi, T. Hambley, H. Freeman. *J. Inorg. Biochem.*, **73**, 173 (1999).